Self-assembling hydrogels based on a complementary host-guest peptide amphiphile pair

Carlos Redondo-Gómez† ⊥, Yamin Abdouni†⊥, C. Remzi Becer†⊥, Alvaro Mata† ⊥*

† School of Engineering & Materials Science, Queen Mary University of London, London E1 4NS, UK
⊥ Institute of Bioengineering, Queen Mary University of London, London E1 4NS, UK

c.redondo@qmul.ac.uk

y.abdouni@qmul.ac.uk

r.becer@qmul.ac.uk

*Corresponding author
Alvaro Mata
a.mata@qmul.ac.uk

ABSTRACT

Supramolecular polymer-based biomaterials play a significant role in current biomedical research. In particular, peptide amphiphiles (PAs) represent a promising material platform for biomedical applications given their modular assembly, tunability, and capacity to render materials with structural and molecular precision. However, the possibility to provide dynamic cues within PA-based materials would increase the capacity to modulate their mechanical and physical properties and consequently enhance their functionality and broader use. In this study, we report on the synthesis of a cationic PA pair bearing complementary adamantane and β-cyclodextrin host-guest cues and their capacity to be further incorporated into self-assembled nanostructures. We demonstrate the possibility of these recognition motifs to selectively bind, enabling noncovalent cross-linking between PA nanofibers, and endowing the resulting low weight (1 wt%) supramolecular hydrogels with enhanced mechanical properties, including stiffness and resistance to degradation, while retaining in vitro biocompatibility. The incorporation of the host-guest PA pairs in the resulting hydrogels allowed not only for macroscopic mechanical control from the molecular scale but also for the possibility to engineer further spatiotemporal dynamic properties, opening opportunities for broader potential applications of PA-based materials.

INTRODUCTION

Over the past decade, supramolecular chemistry has increasingly facilitated the design of a wide variety of functional biomaterials with enhanced precision and versatility.[1,2] In particular, self-assembling approaches offer modularity, tunability, and the possibility to engineer macroscopic properties through molecular modifications.[3] These characteristics arise from the reversible nature of the noncovalent interactions that hold self-assembling biomaterials together, and allows for their ability to assemble in a modular and controllable fashion.[4] Based on these principles, a wide variety of self-assembling systems have been reported based on for example polymers,[5] peptides,[6] proteins,[7] DNA,[8] peptide derivatives,[9] and conjugates of them.[10] Peptide amphiphiles (PAs) are a particularly promising family of self-assembling peptides, which are programmed to assemble in aqueous environments. These molecules comprise a lipid hydrophobic component, a β-sheet forming peptide segment, and charged amino acid residues that provide water-solubility and the possibility to carry bioactive sequences.[11] The dispersive interactions among the hydrophobic tails and the establishment of a hydrogen bonding network between the oligopeptide segments drive the self-assembly processes of PAs in a cooperative fashion, yielding ordered and micrometre-long 1D structures.[12] As the resulting supramolecular network assembles, a nanofibrous hydrogel forms, which can be designed to mimic both structural and functional features of the natural extracellular matrix (ECM).[13] These biomimetic systems have been developed to stimulate specific biological processes such as cell migration[14,15] and differentiation[16] in vitro as well as in vivo regeneration of axons,[17] blood vessels,[18] bone,[19] and cartilage.[20]

Hydrogels are attractive materials for biomedical applications given their molecular-scale control over mechanical and bioresponsive properties.[21,22] While stiffness has been shown to be a key hydrogel parameter to control and drive cell response,[23–25] its tunability remains

challenging. Traditional approaches to tune hydrogel stiffness have mostly relied on modifying either gel concentration or crosslinking density, which can concomitantly modify porosity, network connectivity, and consequently affect bioactivity and degradation.[26] Therefore, other approaches that can selectively control stiffness without affecting other hydrogel parameters would enhance the precision and versatility with which these biomaterials are designed. In particular, supramolecular hydrogels represent an attractive platform to enable such capability due to both the dynamic binding of their molecular components and the weak noncovalent nature of their interactions.[27]

The last three decades have witnessed the use of macrocyclic host-guest interactions to endow materials with dynamic, reversible, and responsive properties.[28] Cyclodextrins (CDs) constitute one of the best studied supramolecular hosts as they exhibit good biocompatibility, degradability, and a wide repertoire of functional groups that render their conjugation with biomacromolecules.[29] The strength and specificity of the CD–guest interaction enables excellent control over material functionality when designing both covalent[30] and supramolecular[31] polymer-based materials. β-Cyclodextrin (β-CD) comprises seven α-D-glucopyranoside units linked by ($\alpha\rightarrow$1,4)-glycosidic bonds, rendering a truncated cone structure with a hydrophilic exterior surface and a hydrophobic interior cavity. This structure is suitable for association with hydrophobic guest motifs of appropriate size and polarity such as adamantane (Ada) derivatives.[29,32–34] A number of CD-Ada peptide-based systems have proven functional as soft materials,[35] delivery devices,[36,37] and chemo-[38] and bio-sensors.[39] However, to our knowledge, both the benefits and functionalities of this host-guest pair have not yet been translated into PA self-assembled hydrogels.

As a strategy to ameliorate the control of mechanical properties of PA hydrogels, we herein report a new family of supramolecular hydrogels prepared through the noncovalent crosslinking between PAs bearing either β-CD or Ada host-guest motifs. We describe the synthesis of both cationic isostructural PA conjugates, the underlying mechanism of both peptide self-assembly and host-guest complexation, as well as the resulting properties of assembled hydrogels. Furthermore, the potential biofunctionality of the system is demonstrated using cell-culture experiments.

EXPERIMENTAL SECTION

Materials. All reagents were purchased from Sigma-Aldrich and used without any further purification unless otherwise stated. Phosphate buffered saline (PBS), Dulbecco's Modified Eagle's Medium (DMEM), Hank's Balanced Salt Solution (HBSS), Penicillin/Streptomycin (P/S), Foetal Bovine Serum (FBS), were obtained from Gibco (Life Technologies).

Circular dichroism (CD). The secondary structure of the PAs was assessed using CD. Peptides were dissolved in water or 4-(2-hydroxyethyl)piperazine-1-ethanesulfonic acid (HEPES) 10 mM saline (155 mM NaCl pH 7.4) at a final concentration of 0.01 wt%, then measured as soon as possible using a 1 mm path-length quartz cuvette in a Pistar-180 spectropolarimeter (Applied Photophysics, Surrey, UK) equipped with a Peltier temperature controller, under a constant nitrogen purging at a constant pressure of 0.7 MPa and temperature of 25 °C. Far UV spectrum were recorded from 190 to 270 nm a wavelength step of 0.5 nm. Each represented spectrum is the average of three consecutive spectra. Temperature variable CD experiments were carried out between 10 ºC and 70 ºC, with a heating rate of 1 ºC/min, and collecting a spectrum every 10 ºC.

Nuclear magnetic resonance (NMR). Mixtures of **Ada-PA** and **βCD-PA** were prepared in D_2O/CD_3OD reaching a final concentration of 10-12 mg/mL. Two dimensional NOESY NMR spectra were recorded on a Bruker AvanceNEO 600 spectrometer at room temperature.

Transmission Electron Microscopy (TEM). PA 0.05 wt% aqueous solutions were imaged after a negative staining treatment. PA samples were drop casted on holey carbon-coated copper TEM grids (Agar Scientific, Stansted, UK), after 5 minutes incubation, solution excess was removed before incubation with 2% uranyl acetate for one minute, grids were then washed with ultrapure water for 30s and air dried for 24h at room temperature before imaging. Bright-field TEM imaging was performed on a JEOL 1230 Transmission Electron Microscope operated at an acceleration voltage of 80 kV. All the images were recorded by a Morada CCD camera (Image Systems) and at least six areas were analysed (corresponding to $n \geq 100$ PA fibers).

Isothermal titration Calorimetry (ITC). ITC experiments were performed at 25 °C using a MicroCal PEAQ-ITC microcalorimeter (Malvern-Panalytical, UK). PA solutions were prepared in previously filtered 10 mM HEPES buffer, pH 7.4. In a typical experiment 19 injections of 2.0 µL titrant were titrated into the sample cell over 2 s with a stirring speed of 750 rpm and 120 s separation to ensure thermal equilibration. Data were baseline adjusted by subtracting background data obtained from equivalent injections of titrant into the buffer solution. The titration curves were analyzed using the integrated public-domain software packages NITPIC, SEDPHAT and GUSSI..

Zeta potential (ξ). PAs were dissolved in MilliQ water, pH values were adjusted by addition of HCl or NH_4OH, transferred to polycarbonate folded capillary cells where zeta potential

measurements were taken in triplicate at 25 °C from pH 3 to 12 using a Zetasizer (Nano-ZS ZEN 3600, Malvern Instruments, UK).

Gel preparation. PAs were dissolved in either water or HEPES buffer, mixed according to the desired **K₃-PA/βCD-PA/Ada-PA** ratio, incubated at 80 °C for 30 min and let to slowly cool down to room temperature, then a 30 µL drop was placed onto a polydimethylsiloxane (PDMS) support, injected 15 µL of PBS 0.1 M and incubated overnight at 25 °C to afford 1 wt% hydrogels in all cases.

Scanning Electron Microscopy (SEM). PA hydrogels were stepwise dehydrated by immersion in increasingly concentrated ethanol solution (25%, 50%, 70%, 80%, 90%, 95%, 100%), for 5 min twice in each solution. Dehydrated samples were dried using a critical point dryer (K850, Quorum Technologies, UK) and gold coated before imaging on an Inspect F50 (FEI Company, the Netherlands) (n ≥ 5).

Epifluorescence Imaging. An inverted epifluorescence widefield Leica DMI4000B microscope (Leica, Germany) equipped with a LEICA DFC300 FX CCD camera was used to visualize FITC (Cyclolab, Hungary) and Nile Red stained peptide aggregates. Peptide solutions were incubated with the fluorescent dye for 30 min at room temperature before imaging and FITC & Texas Red filters were employed.

Rheological measurements. PA hydrogels rheological characterization was performed with a DHR-3 Rheometer (TA Instruments, USA) equipped with an 8 mm diameter parallel plates geometry. Rheological characteristics were monitored by amplitude sweep, frequency sweep, and the self-healing ability of the gels was assessed through creep-recovery tests. G′ (storage

modulus) and G″ (loss modulus) were measured at 25 °C and a constant frequency of 1 Hz in the 0.01% – 10% strain during the amplitude sweep, while the oscillation frequency experiments were carried out at a 0.1% fixed strain along 0.1 – 100 Hz. Creep-recovery tests were performed as follows: an initial 0.1% strain was held for the first 100s, then it was increased to 100% for 100 s, followed by a recovery segment of 0.1% stress for 100 s, the continuous step strains were switched within 200 s for every strain interval.

Degradation/erosion studies. PAs gels were placed in suitable glass vials and incubated in HEPES buffer at 25 ºC. Gels degradation/erosion was determined as reported elsewhere (Figure S7).

Citotoxicity assays. NIH-3T3 fibroblasts were cultured in DMEM supplemented with 10% FBS and 1% P/S in a humidified incubator (37 °C, 5% CO_2). On a typical experiment 5 µL of a 10 mM PA ternary mixture of **K₃-PA/βCD-PA/Ada-PA** (70:15:15) were injected within 50 µL of PBS gelling solution (1 mM PA final concentration). After 30 minutes gelation the excess of PBS was removed and 50,000 NIH-3T3 cells were seeded onto the gels. Gels were kept under orbital agitation for 1 h before static culture for 1, 2 and 7 days. In vitro cell viability was then assessed using the LIVE/DEAD Viability/Cytotoxicity Assay Kit (Molecular Probes), 30 min before imaging hydrogels were incubated in 10 mM Calcein AM and 1 mM ethidium homodimer-1 (EthD-1), stained samples were visualised on an inverted Confocal Laser Scanning Microscope (CLSM) (Leica Laser Scanning Confocal TCS SP2) along with the ImageJ Software (NIH, USA) for reconstructing the 3D images. Cell viability was measured as a ratio of calcein positive cells over total number of cells. All assays were done in at least triplicate.

RESULTS AND DISCUSSION

Design and rationale of supramolecular host-guest nanostructures.

The main goal of this work was to generate a molecularly-designed functional hydrogel that exhibits the benefits of both peptide self-assembly and host-guest interactions. The covalent incorporation of host-guest motifs took place by synthesizing two PA-conjugates bearing either a β-cyclodextrin residue (**βCD-PA**, host-PA) or an adamantane residue (**Ada-PA**, guest-PA). Both **βCD-PA** and **Ada-PA** conjugates are isostructural to the well-characterised cationic **K$_3$-PA**, which we employed as a control. These new host-guest derivatives comprise a hydrophobic palmitoil tail (C$_{16}$-), an oligopeptide motif with a strong tendency to form β-sheets (-V$_3$A$_3$-), an ionizable region that is also responsible for further hydrogelation (-K$_3$-), a triglyine spacer (-G$_3$-) to enhance further fiber display of the host-guest cues, and a 1,2,3-triazole linker that allocated the corresponding β-CD and Ada residues nearby the C-terminus of the respective PA (Scheme 1).
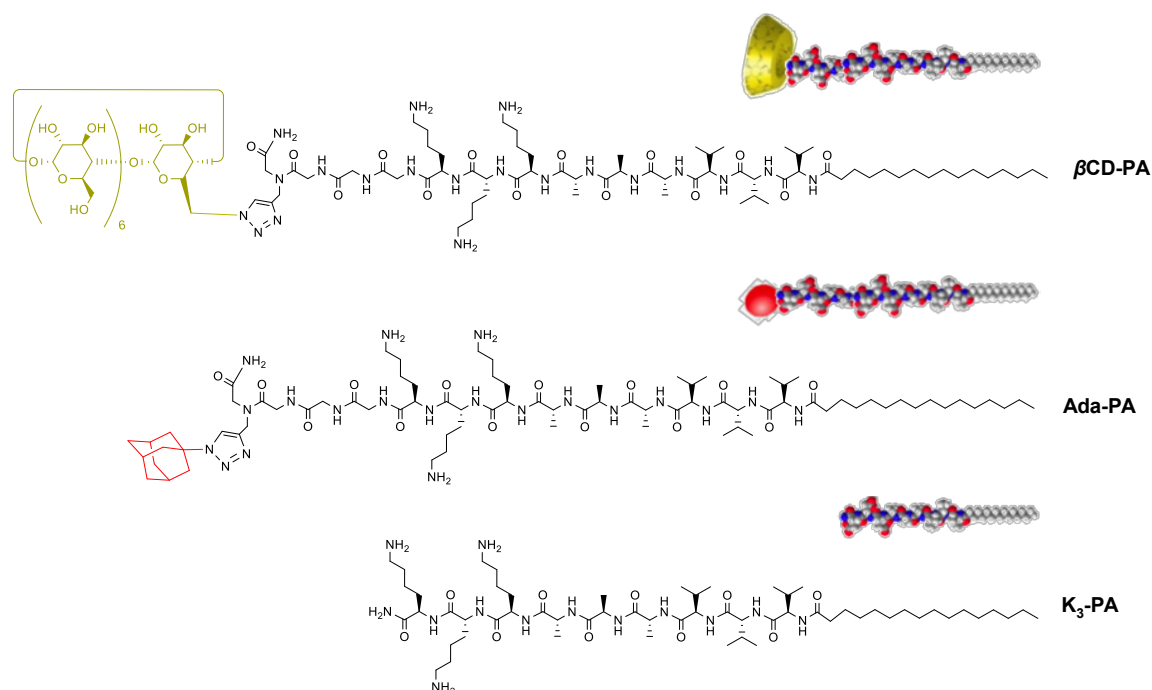
Scheme 1. Molecular structures of the peptide amphiphile (PA) molecules reported in this study. The complementary host-guest PA pair is represented by **βCD-PA** and **Ada-PA**. The

former bears a *β*-cyclodextrin moiety and acts as the host-PA, while the latter bears an

adamantane residue and acts as the guest-PA. Both peptides are isostructural to **K₃-PA**.

Fiber forming individual molecules.

Both ***β*CD-PA** and **Ada-PA** derivatives were synthesised using solid state peptide synthesis

(SSPS) followed by further copper(I)-catalysed alkyne–azide cycloaddition (CuAAC)

coupling,[40] Purification of both peptides and **K₃-PA** was carried out through reverse-phase

High-Performance Liquid Chromatography (RP-HPLC), as acceptable peptide purity was

obtained, a final trifluoroacetic (TFA) removal step was performed and HCl form of all the

PAs was prepared and extensively dialysed for this study. Further synthesis and

characterisation details can be found in the Supporting Information to this paper.

Transmission electron micrographs (TEM) revealed that both host-guest PAs self-assemble

individually into nanofibers when dissolved in water in a micromolar concentration range

(Figure 1B, 1F). While both ***β*CD-PA** and **Ada-PA** exhibited comparable fiber diameters (9.8

± 1.4 nm and 9.6 ± 1.3 nm, respectively) their length varied significantly (184 ± 130 nm and

666 ± 386 nm, respectively) and both exhibited shorted lengths compared to conventional

micrometer-long PA fibers. This length shortening suggests that the allocation of

bulky/hydrophilic *β*-CD or small/hydrophobic Ada residues on the surface of the PA

nanostructures may originate packing disruptions, resulting in shorter self-assembled fibers.

Despite this potential intrusion in fiber formation, zeta potential (ξ) measurements revealed

that both self-assembled ***β*CD-PA** and **Ada-PA** fibers exhibit a net positive charge along a

wide range of pH values, suggesting that the presence of the host-guest motifs does not

intrude on the surface display of the positively charged lysine residues once the fibers have

assembled (Figure 1D, 1H).

βCD-PA secondary structure in water and HEPES.

It is agreed that the assembly of PAs into fibers in aqueous environments is driven by both the hydrophobic association of the alkyl tail and the cohesive formation of a regular hydrogen bonding network (*i.e.* β-sheets). Interestingly, circular dichroism (CD) measurements revealed that **βCD-PA** fibers do not attain the expected β-sheets in water at 25 ºC (Figure 1A, Figure S5) but rather a β-turn-like secondary structure.[41] Compared to a classical PA such as **K₃-PA**,[42] the geometrical packing parameters in **βCD-PA** have been modified by the presence of the voluminous β-CD motifs at the C-terminus. We speculate that allocating these moieties at the surface of the self-assembled nanofibers could restrict the peptide backbone and promote the observed β-turn conformation (Figure 1A) as reported in dipalmitoylated PA systems.[43] Interestingly, these β-turns could be switched to a random coil conformation when assembled at room temperature and under physiological conditions (*i.e.* in HEPES pH 7.4, [NaCl] = 0.9 wt%), maintaining a fibrous morphology and exhibiting a slight tendency to form bundles (Figure 1A, 1C; Figure S5).
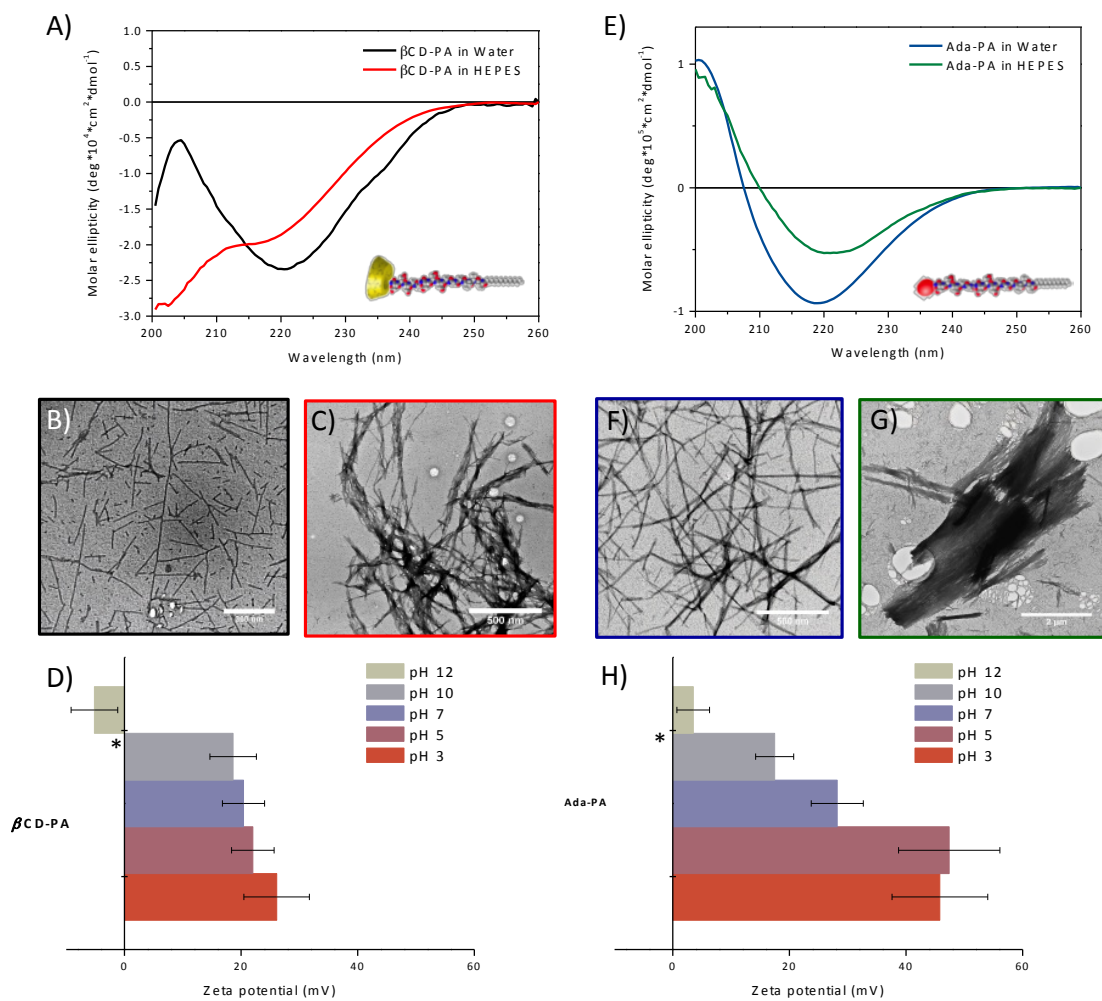
Figure 1. Self-assembly of *β***CD-PA** and **Ada-PA** into nanofibers in aqueous media. A) Circular dichroism (CD) spectra and B) transmission electron microscopy (TEM) images of *β***CD-PA** [38 µM] in water (black) and C) HEPES buffer (red). D) Zeta potential (ξ) measurements of solutions of *β*CD-PA in water (n = 3, mean ± s.d.). E) CD spectra and F) TEM micrographs of **Ada-PA** [63 µM] in water (blue) and G) HEPES buffer (green). H) Zeta potential (ξ) measurements of solutions of **Ada-PA** in water (n = 3, mean ± s.d., * marks the PA isoelectric point in each case).

Ada-PA secondary structure in water and HEPES.

In contrast, CD investigations revealed that **Ada-PA** nanofibers exhibited well-defined *β*-sheet conformations in both water and HEPES buffer (Figure 1E). TEM micrographs

revealed that while single **Ada-PA** fibers exist in water and HEPES buffer at low concentration regimes (Figure S3), at higher concentrations these fibers tend to bundle into small fibrils, that eventually appear to coalesce into larger raft-like objects of heterogeneous morphology and size (Figure 1G, Figure S4), similar to the nanosheets reported by Chen et al.[44] We speculate that these structures form through van der Waals interactions amid adjacent Ada residues, however, confirmation of this hypothesis will require investigations beyond the scope of this study.

Both **Ada-PA** and **βCD-PA** exhibited temperature-driven conformational changes in accordance to previous studies,[45] Figure S5 shows our system might retain a substantial content of their native secondary structure at physiologically relevant conditions. These results demonstrate that incorporation of small hydrophobic moieties in **Ada-PA** fibers does not affect the peptide backbone conformation in aqueous environments, but can lead to fiber bundling at higher concentration regimes.

Supramolecular decoration of *β*CD-PA and Ada-PA nanofibers.

As host-guest motifs are presented on the surface of both **βCD-PA** and **Ada-PA** nanostructures, these cues elicit the formation of inclusion complexes with free complementary partners in solution. When **βCD-PA** nanofibers were incubated with rimantadine in HEPES buffer, the formation of a well-known 1:1 inclusion complex took place between self-assembled β-CD units and free Ada moieties in solution. TEM micrographs revealed that this noncovalent interaction has no significant impact on fiber morphology (Figure 2B), but CD studies indicated that the **βCD-PA** undergoes a conformational change from a random coil to a β-sheet conformation upon binding Ada units (Figure 2A). To further investigate whether these inclusion complexes can be formed at the

surface of self-assembled **Ada-PA**, isothermal titration calorimetry (ITC) experiments were performed. Titration of assembled **Ada-PA** nanofibers with free *β*-CD revealed a 1:1 binding mode (Figure S6, Table 1), same evidence was collected through Nuclear Overhauser effect spectroscopy (NOESY) (Figure S7), while TEM micrographs showed that this noncovalent complexation had little effect on fiber morphology (Figure 2D). Furthermore, CD studies revealed that the **Ada-PA** undergoes a conformational change when binding to free *β*-CD moieties, switching from *β*-sheet to random coil (Figure 2C). These results suggest that host-guest complexations could be used as a tool to tune peptide conformations with little morphological alterations on the resulting self-assembled nanostructures. Moreover, this platform widens the possibility to decorate self-assembled peptide nanostructures with suitable host-guest partners bearing bioactive motifs,[46,47] thus providing new modular assembly of biomaterials with increasing complexity and functionality beyond traditional covalent approaches.
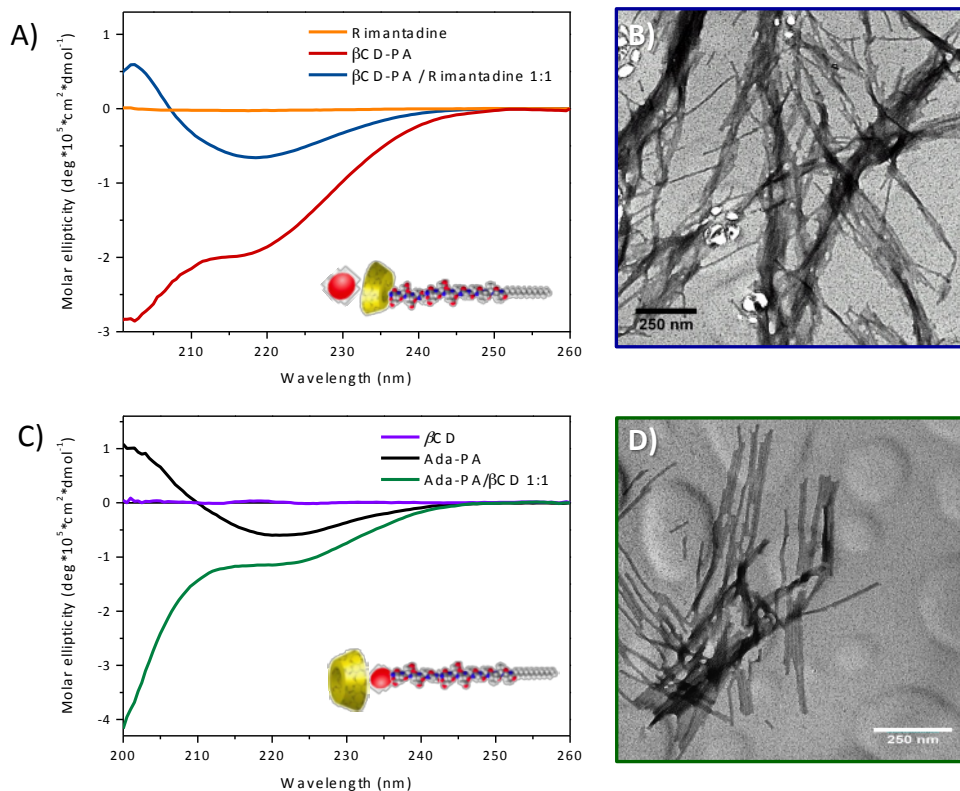
Figure 2. Noncovalent decoration of **βCD-PA** and **Ada-PA** fibers with complementary host/guest motifs in HEPES buffer. A) Circular dichroism (CD) spectra of an equimolar mixture of **βCD-PA** and rimantadine and B) transmission electron microscopy (TEM) micrograph of the resulting nanofibers [38 μM, blue]. C) CD spectra of an equimolar mixture of **Ada-PA** and β-cyclodextrin, and D) TEM micrograph of the resulting nanofibers [63 μM, green].

βCD-PA and Ada-PA interacting with each other.

After confirming that both **βCD-PA** and **Ada-PA** can form inclusion complexes with their complementary partners in solution, we proceeded to assess the noncovalent binding between these two host-guest PAs. ITC titrations revealed that both **βCD-PA** and **Ada-PA** bind to each other following a 1:1 stoichiometry (N), exhibiting a dissociation constant (K_D) of 13.2 ± 4.4 μM as well as enthalpic, entropic and free energy values similar to those of **Ada-PA** titrated with free β-CD (Figure 3A, Table 1).[36,48] Nuclear Overhauser effect spectroscopy (NOESY) experiments revealed cross-peaks between the signals at 3 - 4.5 ppm assigned to the inner protons of βCD and the signals at 1.5 - 2.2 ppm assigned to Ada. This result demonstrates the allocation of Ada residues into the cavity of their complementary β-CD partners, resulting in the formation of the noncovalent **βCD-PA•Ada-PA** complex (Figure S8).[48] CD spectroscopy confirmed that the noncovalent **βCD-PA•Ada-PA** complex exhibits different secondary structures in water and HEPES buffer, forming β-sheets and β-turn-like structures, respectively (Figure 3B). This difference in conformation is expected, as isostructural systems to ours exhibit conformational transitions when ionic strength is increased.[49] Nonetheless, TEM micrographs of equimolar mixtures of **βCD-PA** and **Ada-PA** demonstrated that their binding did not unsettle fiber formation (Figure 3C, 3D), thus

indicating that they can be incorporated into a PA hydrogel without compromising its fibrous structure.

Table 1. Thermodynamic parameters associated to the host-guest interactions of *β*CD / Ada-PA and *β*CD-PA / Ada-PA systems.

System	N	K_D (µM)	Ka (M^{-1})	ΔH (kJ•mol^{-1})	ΔG (kJ•mol^{-1})	-TΔS (kJ•mol^{-1})
*β*CD / Ada-PA	0.95 ± 0.07	25.6 ± 6.4	(3.91 ± 0.98) x 10^4	-14.56 ± 2.3	-26.23	-11.67
*β*CD-PA / Ada-PA	1.02 ± 0.05	13.2 ± 4.4	(7.6 ± 2.5) x10^4	-9.41 ± 0.84	-27.87	-18.45

_β_CD-PA and Ada-PA assemblies within hydrogels.

A main objective of the study was to generate **_β_CD-PA•Ada-PA** complexes that would allow noncovalent tethering between PA-fibers, resulting in hydrogel networks with improved structural integrity. In order to provide further tunability of these tethering interactions, we self-assembled both **_β_CD-PA** and **Ada-PA** in the presence of the cationic **K₃-PA**, which permits control over the spacing and concentration of both **_β_CD-PA** and **Ada-PA**. It is reported that heating **K₃-PA** solutions to 80 ºC and then gently cooling them down can lead to lengthening of subsequently self-assembled nanofibers.[12] Furthermore, scaffolds made from such longer PA fibers consist of long bundled fibers, that can lead to improved spreading and proliferation of cells.[49,50] Consequently, mixtures of **_β_CD-PA**, **Ada-PA,** and an excess of **K₃-PA** were carefully prepared and thermally treated to obtain longer and more cytocompatible PA fibers. SEM micrographs of hydrogels composed of **K₃-PA** and identical increasing content of **_β_CD-PA** and **Ada-PA**, revealed that the presence of the host-guest PAs neither caused phase separation in the resulting hydrogels nor disturbed the morphology or

dimensions of the fibrillar nanostructures (Figure 3F). This PA gel-forming network preservation in presence of *β*CD/Ada joints demonstrated the possibility to use them as interfiber cross-linking cues within a PA-hydrogel (Figure 3G).
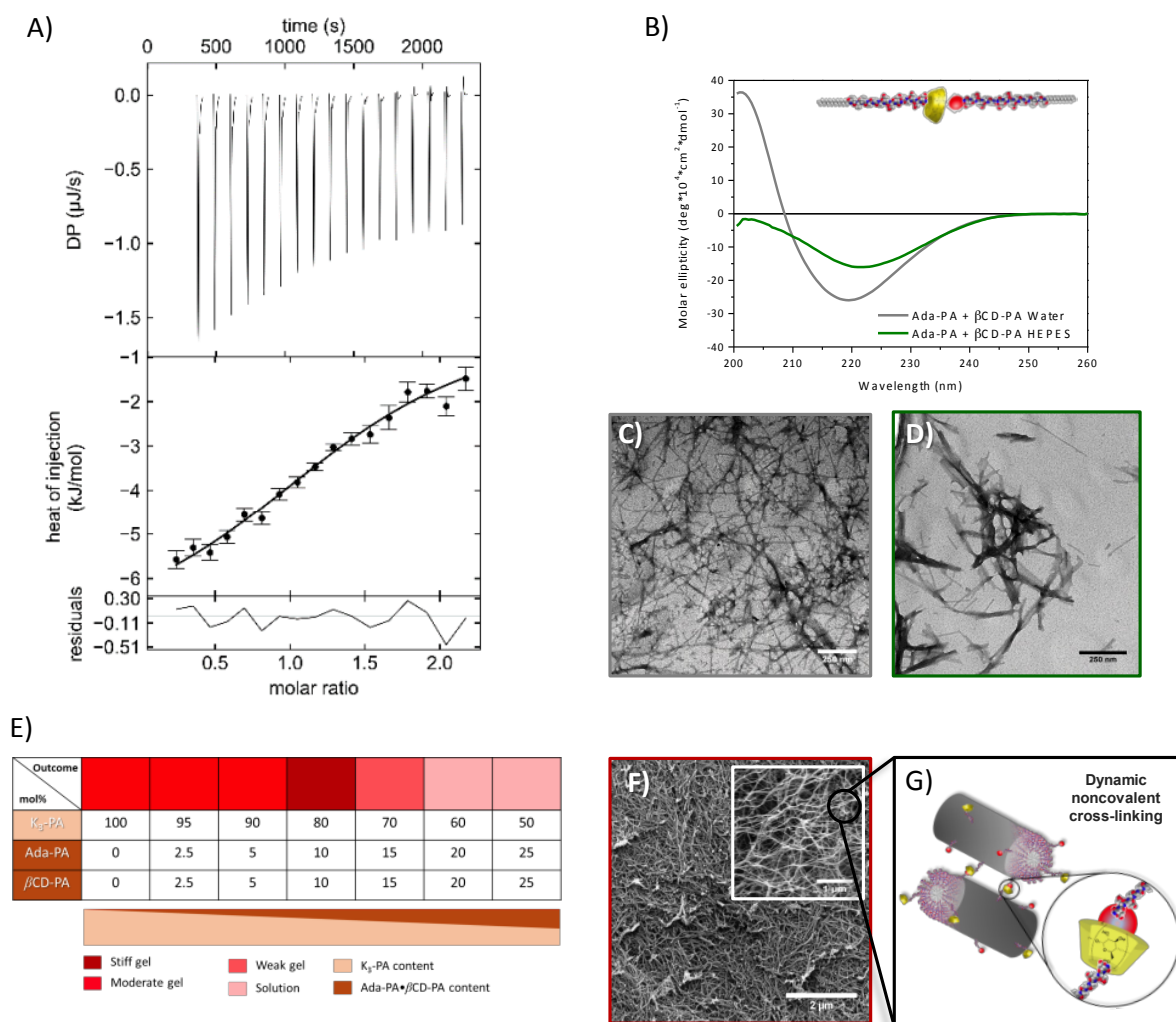

Figure 3. Molecular binding between *β*CD-PA and Ada-PA. A) Isothermal titration Calorimetry (ITC) titration of **Ada-PA** with ***β*CD-PA** evidencing the formation of a 1:1 host-guest inclusion complex ([**Ada-PA**] = 75 µM, [***β*CD-PA**] = 600 µM, T = 25°C, 19x10 µL injections). B) Circular dichroism (CD) spectra and transmission electron microscopy (TEM) micrographs of equimolar mixtures of **Ada-PA** and ***β*CD-PA** in C) water and D) HEPES buffer. E) Heat map showing the relative strength of different **K₃-PA/*β*CD-PA•Ada-PA** hydrogels. F) Scanning electron micrographs (SEMs) of a **K₃-PA/*β*CD-PA•Ada-PA**

80:10:10 mol% hydrogel demonstrating the persistence of a fibrous network after the noncovalent binding of βCD and Ada motifs. G) Schematics illustrating the underlying host-guest interaction mechanism between PA nanofibers.

Stiffness of βCD-PA and Ada-PA hydrogels.

Given these results, we reasoned that **K₃-PA** gels containing increasing content of **βCD-PA** and **Ada-PA** would increase in stiffness as more interfiber binding takes place. To confirm this possibility, the stiffness and response to deformation of the hydrogels were assessed through dynamic rheology. Amplitude and frequency sweep experiments were used to quantify the storage modulus (G') and loss modulus (G'') of **K₃-PA/βCD-PA•Ada-PA** 1 wt% hydrogels containing increasing fractions of host-guest PAs (90:5:5, 80:10:10, and 70:15:15 mol%) (Figure 4A, Figure S9). Control **K₃-PA** hydrogels exhibited G' values of 2.8 ± 0.5 kPa while **K₃-PA/βCD-PA•Ada-PA** hydrogels displayed higher G' and G'' values (Figure 4A). Values for both G' and G'' increased with the concentration of the **βCD-PA•Ada-PA** pair in the hydrogels, gel stiffness increased significantly (compared to control **K₃-PA** hydrogels) until reaching a maximum of 5.1 ± 0.8 kPa when the fractions of **βCD-PA** and **Ada-PA** were 10 mol% each (80:10:10 gels, p < 0.0001, n > 3, Table S3). Increasing **βCD-PA•Ada-PA** pair concentration above 10 mol% was detrimental for hydrogel stiffness. Hydrogels containing **K₃-PA/βCD-PA•Ada-PA** 70:15:15 mol% exhibited a similar stiffness as **K₃-PA** control gels, while mixtures incorporating higher ratios of the host-guest pair than 70:15:15 mol% rendered only solutions in presence of the PBS gellator, most likely due to a decrease in nanofiber length (Figure 3E, 3D). Nonetheless, neither **K₃-PA/βCD-PA** nor **K₃-PA/Ada-PA** binary hydrogels exhibited an increase in stiffness compared to control **K₃-PA** ones assembled at the same 1 wt% concentration (Figure S10). This suggests that the host−guest binding between nanofibers bearing **βCD-PA** and those bearing **Ada-PA** is likely

responsible for the observed increase in stiffness in the ternary gels. Other approaches aiming to modulate PA hydrogel stiffness rely on modification of their intrafiber hydrogen bonding network strength,[51] pH,[52] concentration,[52] covalent capture via hydrophobic domains,[15] covalent interfiber crosslinking[53] or mixing with other PAs,[54] proteins,[55,56] phospholipids,[57] and metal counterions.[58] On the other hand, our non-covalent crosslinking approach allows for enhancing stiffness without altering other gel parameters such as peptide concentration and porosity. On top of these benefits, the integration of dynamic host-guest chemistry into supramolecular PA hydrogels allows for the possibility to engineer further temporal and morphological properties, which are relevant within cell environments.[22]

Self-healing and resistance to degradation of βCD-PA and Ada-PA hydrogels.

In addition to enhancing gel stiffness, we hypothesized that the precise and reversible nature of the host-guest interactions would elicit additional effects on the structural integrity of the **K₃-PA/βCD-PA•Ada-PA** hydrogels. First, given the supramolecular and noncovalent nature of these materials,[52] we tested the self-healing and shear-thinning properties of the hydrogels by step strain measurements. When undergoing changes from large (100%) to small (0.10%) strain values, the hydrogels exhibited a reversible gel-sol transition and rapidly recovered up to 90% of their G' and G'' after sheared for up to 4 cycles (Figure 4B). **K₃-PA/βCD-PA•Ada-PA** hydrogels proved to withstand more damage than control **K₃-PA** hydrogels under the same exhibited strain, but were also able to recover in a similar way to the control gels (Figure S11). In addition, we tested the effect of the host-guest motifs on the stability of the PA hydrogels upon degradation when incubated in HEPES at 25 ºC. In this fashion, weight remaining ratios was monitored after exhaustive removal of buffer and determination of the residual hydrogel mass (Figure S12).[59] The results indicate that 70:15:15 mol% **K₃-PA/βCD-PA•Ada-PA** hydrogels are able to withstand this buffer exchange process for up to

7 weeks before full degradation compared to **K$_3$-PA**, which completely degraded after 2 weeks (Figure 4C). It can be speculated that the host-guest interfiber tethering sites provide an additional anchoring force that confines individual PA molecules to the fibrillar hydrogel network, decreasing Fickian diffusion of free PA-molecules, thus slowing the rate of gel erosion.[60] These results not only demonstrate that the *β*CD/Ada system enhances the stability of PA hydrogels by helping to preserve their structural integrity, but also allows for the tuning of their time-dependent properties, which could be of use when present in tissue regeneration and development sites.[22]
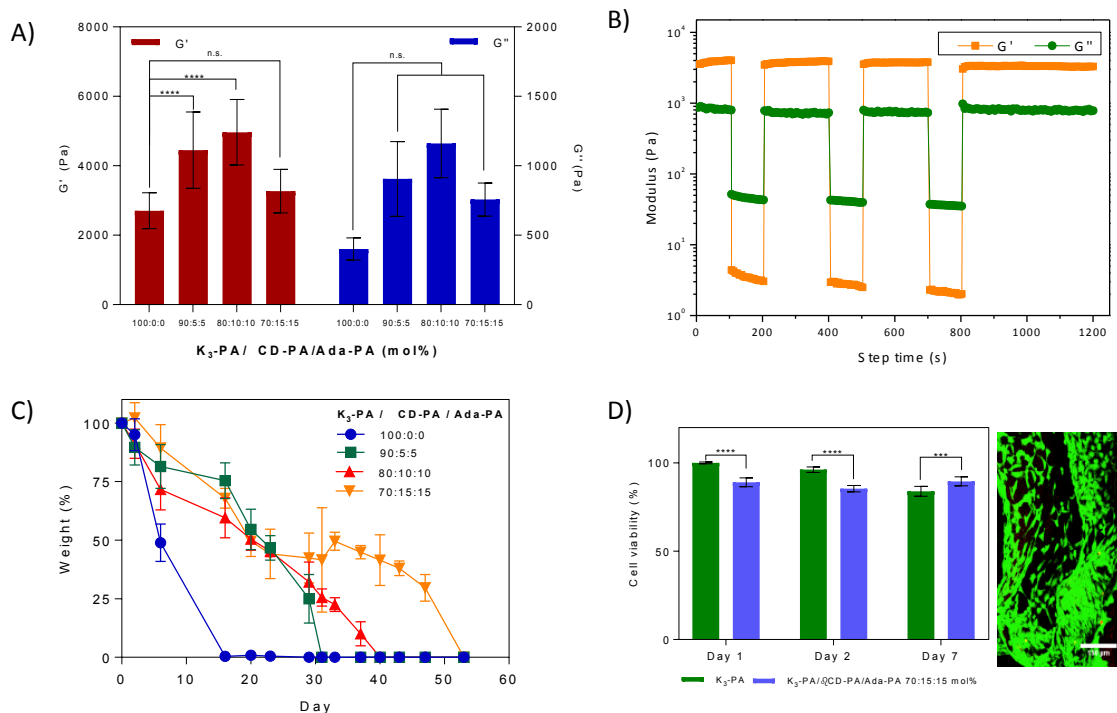

Figure 4. Co-assembling of *β*CD-PA and **Ada-PA** into a functional hydrogel with improved properties. A) Storage (G') and loss (G'') moduli values of different **K$_3$-PA/Ada-PA•*β*CD-PA** hydrogels (1 wt%) determined by oscillatory rheology (see text, **** $p < 0.0001$, n.s. no significant difference, $n > 3$). B) G' (blue) and G'' (red) of a **K$_3$-PA/Ada-PA•*β*CD-PA** 80:10:10 mol% hydrogel in continuous step strain measurements (1 wt%, T = 25 ºC). Large strains (100 %) inverted the G' and G'' values to render the sol state. On the other hand, G'

was recovered under small strains (0.1 %) within less than 30 s. C) Degradation profile of **K₃-PA/Ada-PA•βCD-PA** hydrogels in time. Weight remaining ratios of 90:5:5, 80:10:10 and 70:15:15 mol% hydrogels as well as **K₃-PA** control hydrogels are shown. D) Cell viability determinations of NIH-3T3 fibroblasts cultured onto **K₃-PA/Ada-PA•βCD-PA** 70:15:15 mol% hydrogels (red), **K₃-PA** gels were used as controls (blue, 1 wt% in both cases) (**** $p < 0.0001$, *** $p < 0.001$, $n > 3$) Inset: LIVE-DEAD image from the host-guest based hydrogels at day 7 (green: calcein AM, alive cells; red: ethidium homodimer-1 (EthD-1), dead cells).

Biocompatibility of βCD-PA and Ada-PA hydrogels.

To assess the potential of our modified PA hydrogels to be used in biological applications, NIH-3T3 fibroblasts were cultured on either **K₃-PA/βCD-PA•Ada-PA** or **K₃-PA** control hydrogels for up 7 days. Cells attached and exhibited a spread morphology on both hydrogel systems after two days (Figure S13), and cells seeded on **K₃-PA** control gels showed higher viability at this point. However, on day 7, cells growing on **K₃-PA/βCD-PA•Ada-PA** hydrogels exhibited higher viability (89.6 ± 2.6 %) compared to cells growing on **K₃-PA** controls (83.9 ± 2.8 %) (Figure 4D). We speculate that the host-guest motifs play a role in partially shielding the positive charges from the cationic nanofibers, in fact, NIH-3T3 fibroblasts viability assays in solution showed higher cell survival in **βCD-PA** than **K₃-PA** (Figure S14). Also, the noncovalent interfiber binding leads to obtaining stiffer hydrogels, which could promote the expression of mechanosensitive proteins.[25] It is possible that this observed increased cell viability observed in our **K₃-PA/βCD-PA•Ada-PA** hydrogels after 7 days of culture results from a stiffer gel as a result of our host guest interaction, studies have reported an effect on increasing cell viability as a result of matrix stiffness.[61] It is noteworthy that our approach enables an increase in stiffness without affecting nanofiber density (as total

amount of self-assembling PAs remain constant), therefore, network crosslinking and cell microenvironments shall remain similar to those of conventional **K$_3$-PA** gels, in terms of cell nutrient access, gas exchange and other physiological parameters. This capacity could have a significant effect on cell function, for instance cell differentiation.[62] Taking advantage of the capacity to modulate supramolecular hydrogel properties as a result of our host-guest approach, further optimisation of the hydrogel stiffness would be possible, but it might depend on specific cell type behaviours and therapeutic use. It is noteworthy that when cells were embedded within the hydrogel materials, a significant decrease in viability was observed in both **K$_3$-PA/βCD-PA•Ada-PA** and **K$_3$-PA** controls hydrogels. This effect is likely a result of the positively charged PAs used, as it is well-known that cationic peptides cytotoxicity can be tuned.[63,64]

CONCLUSIONS

In this study, we report on the synthesis, supramolecular aggregation, and structural improvement of a new family of PA hydrogels based on the dynamic noncovalent binding of β-cyclodextrin and adamantane motifs. Through this approach, we aim to develop a robust and versatile noncovalent cross-linking strategy for peptide-based biomaterials. The work validated the possibility to incorporate host-guest binding motifs on self-assembling PA molecules to generate hydrogel biomaterials with enhanced stiffness and structural integrity without altering parameters such as total peptide concentration. To validate the applicability of the biomaterial, we showed that the system can be assembled with different PA molecules and serve as substrates for in vitro cell-culture. Our study demonstrates that host-guest interactions represent an attractive and viable tool to not only improve mechanical and structural features in PA-based hydrogels, but also to further incorporate dynamic guests and

structural complexity levels of PA hydrogels. The system may find applications in the development of novel therapies for disease and regenerative medicine.

References

(1)   Tu, Y.; Peng, F.; Adawy, A.; Men, Y.; Abdelmohsen, L. K. E. A.; Wilson, D. A. Mimicking the Cell: Bio-Inspired Functions of Supramolecular Assemblies. *Chem. Rev.* **2016**, *116* (4), 2023–2078. https://doi.org/10.1021/acs.chemrev.5b00344.

(2)   Zhang, S. Fabrication of Novel Biomaterials through Molecular Self-Assembly. *Nat. Biotechnol.* **2003**, *21* (10), 1171–1178. https://doi.org/10.1038/nbt874.

(3)   Mann, J. L.; Yu, A. C.; Agmon, G.; Appel, E. A. Supramolecular Polymeric Biomaterials. *Biomater. Sci.* **2018**, *6* (1), 10–37. https://doi.org/10.1039/c7bm00780a.

(4)   Webber, M. J.; Appel, E. A.; Meijer, E. W.; Langer, R. Supramolecular Biomaterials. *Nat. Mater.* **2015**, *15* (1), 13–26. https://doi.org/10.1038/nmat4474.

(5)   Highley, C. B.; Rodell, C. B.; Burdick, J. A. Direct 3D Printing of Shear-Thinning Hydrogels into Self-Healing Hydrogels. *Adv. Mater.* **2015**, *27* (34), 5075–5079. https://doi.org/10.1002/adma.201501234.

(6)   Wu, E. C.; Zhang, S.; Hauser, C. A. E. Self-Assembling Peptides as Cell-Interactive Scaffolds. *Adv. Funct. Mater.* **2012**, *22* (3), 456–468. https://doi.org/10.1002/adfm.201101905.

(7)   Luo, Q.; Hou, C.; Bai, Y.; Wang, R.; Liu, J. Protein Assembly: Versatile Approaches to Construct Highly Ordered Nanostructures. *Chem. Rev.* **2016**, *116* (22), 13571–13632. https://doi.org/10.1021/acs.chemrev.6b00228.

(8)   Wang, Z. G.; Ding, B. DNA-Based Self-Assembly for Functional Nanomaterials. *Adv. Mater.* **2013**, *25* (28), 3905–3914. https://doi.org/10.1002/adma.201301450.

(9)   Enzyme-Assisted Self-Assembly under Thermodynamic Control. *Nat. Nanotechnol.* **2009**, *4* (1), 19–24. https://doi.org/10.1038/nnano.2008.378.

(10)   Freeman, R.; Han, M.; Álvarez, Z.; Lewis, J. A.; Wester, J. R.; Stephanopoulos, N.; McClendon, M. T.; Lynsky, C.; Godbe, J. M.; Sangji, H.; Luijten, E.; Stupp, S. I. Reversible Self-Assembly of Superstructured Networks. *Science (80-.).* **2018**, *362* (6416), 808–813. https://doi.org/10.1126/science.aat6141.

(11)   Hartgerink, J. D.; Beniash, E.; Stupp, S. I. Self-Assembly and Mineralization of Peptide-Amphiphile Nanofibers. *Science (80-.).* **2011**, *1684* (2001), 1684–1688. https://doi.org/10.1126/science.1063187.

(12)   Hendricks, M. P.; Sato, K.; Palmer, L. C.; Stupp, S. I. Supramolecular Assembly of Peptide Amphiphiles. *Acc. Chem. Res.* **2017**, *50* (10), 2440–2448. https://doi.org/10.1021/acs.accounts.7b00297.

(13)   Ferreira, D. S.; Marques, A. P.; Reis, R. L.; Azevedo, H. S. Hyaluronan and Self-Assembling Peptides as Building Blocks to Reconstruct the Extracellular Environment in Skin Tissue. *Biomater. Sci.* **2013**, *1* (9), 952–964. https://doi.org/10.1039/c3bm60019j.

(14)   de la Cruz, M. O.; Mantei, J. R.; Palmer, L. C.; Bitton, R.; Greenfield, M. A.; Zhang, S.; Stupp, S. I.; Aparicio, C.; Mata, A. A Self-Assembly Pathway to Aligned Monodomain Gels. *Nat. Mater.* **2010**, *9* (7), 594–601. https://doi.org/10.1038/nmat2778.

(15)   Mata, A.; Hsu, L.; Capito, R.; Aparicio, C.; Henrikson, K.; Stupp, S. I. Micropatterning of Bioactive Self-Assembling Gels. *Soft Matter* **2009**, *5* (6), 1228–1236. https://doi.org/10.1039/b819002j.

(16)   Silva, G. A.; Czeisler, C.; Niece, K. L.; Beniash, E.; Harrington, D. A.; Kessler, J. A.; Stupp, S. I. Selective Differentiation of Neural Progenitor Cells by High-Epitope Density Nanofibers. *Science (80-.).* **2004**, *303* (5662), 1352–1355. https://doi.org/10.1126/science.1093783.

(17)   McClendon, M. T.; Yalom, A.; Berns, E. J.; Hokugo, A.; Stupp, S. I.; Jarrahy, R.; Spigelman, I.; Li, A.; Stephanopoulos, N.; Segovia, L. A. A Bioengineered Peripheral Nerve Construct Using Aligned Peptide Amphiphile Nanofibers. *Biomaterials* **2014**, *35* (31), 8780–8790. https://doi.org/10.1016/j.biomaterials.2014.06.049.

(18)   Newcomb, C. J.; Webber, M. J.; Tongers, J.; Losordo, D. W.; Bauersachs, J.; Stupp, S. I.; Marquardt, K.-T. Supramolecular Nanostructures That Mimic VEGF as a Strategy for Ischemic Tissue Repair. *Proc. Natl. Acad. Sci.* **2011**, *108* (33), 13438–13443. https://doi.org/10.1073/pnas.1016546108.

(19)   Stock, S. R.; Henrikson, K. J.; Geng, Y.; Mata, A.; Stupp, S. I.; Satcher, R. L.; Aparicio, C. Bone Regeneration Mediated by Biomimetic Mineralization of a

Nanofiber Matrix. *Biomaterials* **2010**, *31* (23), 6004–6012. https://doi.org/10.1016/j.biomaterials.2010.04.013.

(20) Hsieh, C.; Shah, R. N.; Del Rosario Lim, M. M.; Stupp, S. I.; Nuber, G.; Shah, N. A. Supramolecular Design of Self-Assembling Nanofibers for Cartilage Regeneration. *Proc. Natl. Acad. Sci.* **2010**, *107* (8), 3293–3298. https://doi.org/10.1073/pnas.0906501107.

(21) Peppas, N. A.; Hilt, J. Z.; Khademhosseini, A.; Langer, R. Hydrogels in Biology and Medicine: From Molecular Principles to Bionanotechnology. *Adv. Mater.* **2006**, *18* (11), 1345–1360. https://doi.org/10.1002/adma.200501612.

(22) Burdick, J. A.; Murphy, W. L. Moving from Static to Dynamic Complexity in Hydrogel Design. *Nat. Commun.* **2012**, *3*, 1–8. https://doi.org/10.1038/ncomms2271.

(23) Rehfeldt, F.; Engler, A. J.; Eckhardt, A.; Ahmed, F.; Discher, D. E. Cell Responses to the Mechanochemical Microenvironment-Implications for Regenerative Medicine and Drug Delivery. *Adv. Drug Deliv. Rev.* **2007**, *59* (13), 1329–1339. https://doi.org/10.1016/j.addr.2007.08.007.

(24) Huebsch, N.; Mooney, D. J.; Klumpers, D.; Duda, G. N.; Darnell, M.; Chaudhuri, O.; Weaver, J. C.; Lee, H.; Gu, L.; Bencherif, S. A.; Lippens, E. Hydrogels with Tunable Stress Relaxation Regulate Stem Cell Fate and Activity. *Nat. Mater.* **2016**, *15* (3), 326–334. https://doi.org/10.1038/nmat4489.

(25) Kennedy, B. F.; McFetridge, M. L.; Sampson, D. D.; Engler, A. J.; Vo, B.-N.; Bieback, K.; Young, J. L.; Taylor-Weiner, H.; Kim, D. Y.; Holle, A. W.; Wijesinghe, P.; Choi, Y. S.; Wen, J. H.; Lee, A. R.; Spatz, J. P.; Hadden, W. J. Stem Cell Migration and Mechanotransduction on Linear Stiffness Gradient Hydrogels. *Proc. Natl. Acad. Sci.* **2017**, *114* (22), 5647–5652. https://doi.org/10.1073/pnas.1618239114.

(26) Zhang, Y. S.; Khademhosseini, A. Advances in Engineering Hydrogels. *Science (80-.*

). **2017**, *356* (6337). https://doi.org/10.1126/science.aaf3627.

(27) Mantooth, S. M.; Munoz-Robles, B. G.; Webber, M. J. Dynamic Hydrogels from Host–Guest Supramolecular Interactions. *Macromol. Biosci.* **2019**, *19* (1), 1–12. https://doi.org/10.1002/mabi.201800281.

(28) Yang, H.; Yuan, B.; Zhang, X.; Scherman, O. A. Supramolecular Chemistry at Interfaces: Host-Guest Interactions for Fabricating Multifunctional Biointerfaces. *Acc. Chem. Res.* **2014**, *47* (7), 2106–2115. https://doi.org/10.1021/ar500105t.

(29) Schmidt, B. V. K. J.; Barner-Kowollik, C. Dynamic Macromolecular Material Design—The Versatility of Cyclodextrin-Based Host–Guest Chemistry. *Angew. Chemie - Int. Ed.* **2017**, *56* (29), 8350–8369. https://doi.org/10.1002/anie.201612150.

(30) Nakahata, M.; Takashima, Y.; Yamaguchi, H.; Harada, A. Redox-Responsive Self-Healing Materials Formed from Host-Guest Polymers. *Nat. Commun.* **2011**, *2* (1), 511–516. https://doi.org/10.1038/ncomms1521.

(31) Harada, A.; Takashima, Y.; Nakahata, M. Supramolecular Polymeric Materials via Cyclodextrin-Guest Interactions. *Acc. Chem. Res.* **2014**, *47* (7), 2128–2140. https://doi.org/10.1021/ar500109h.

(32) Abdouni, Y.; Yilmaz, G.; Becer, C. R. Sequence Controlled Polymers from a Novel β-Cyclodextrin Core. *Macromol. Rapid Commun.* **2017**, *38* (24), 1700501. https://doi.org/10.1002/marc.201700501.

(33) Zhang, Q.; Su, L.; Collins, J.; Chen, G.; Wallis, R.; Mitchell, D. A.; Haddleton, D. M.; Becer, C. R. Dendritic Cell Lectin-Targeting Sentinel-like Unimolecular Glycoconjugates to Release an Anti-HIV Drug. *J. Am. Chem. Soc.* **2014**, *136* (11), 4325–4332. https://doi.org/10.1021/ja4131565.

(34) Yilmaz, G.; Uzunova, V.; Napier, R.; Becer, C. R. Single-Chain Glycopolymer Folding via Host-Guest Interactions and Its Unprecedented Effect on DC-SIGN

Binding. *Biomacromolecules* **2018**, *19* (7), 3040–3047. https://doi.org/10.1021/acs.biomac.8b00600.

(35)   Lin, Y. C.; Wang, P. I.; Kuo, S. W. Water-Soluble, Stable Helical Polypeptide-Grafted Cyclodextrin Bioconjugates: Synthesis, Secondary and Self-Assembly Structures, and Inclusion Complex with Guest Compounds. *Soft Matter* **2012**, *8* (37), 9676–9684. https://doi.org/10.1039/c2sm25804h.

(36)   Versluis, F.; Voskuhl, J.; Stuart, M. C. A.; Bultema, J. B.; Kehr, S.; Ravoo, B. J.; Kros, A. Power Struggles between Oligopeptides and Cyclodextrin Vesicles. *Soft Matter* **2012**, *8* (33), 8770–8777. https://doi.org/10.1039/c2sm26090e.

(37)   Xue, S.-S.; Ye, R.-R.; Mao, Z.-W.; Ji, L.-N.; Tan, C.-P.; Cao, J.-J.; Chen, M.-H.; Zhang, D.-Y. Tumor-Targeted Supramolecular Nanoparticles Self-Assembled from a Ruthenium-β-Cyclodextrin Complex and an Adamantane-Functionalized Peptide. *Chem. Commun.* **2017**, *53* (5), 842–845. https://doi.org/10.1039/c6cc08296c.

(38)   Hossain, M. A.; Hamasaki, K.; Takahashi, K.; Mihara, H.; Ueno, A. Guest-Induced Diminishment in Fluorescence Quenching and Molecule Sensing Ability of a Novel Cyclodextrin-Peptide Conjugate [7]. *J. Am. Chem. Soc.* **2001**, *123* (30), 7435–7436. https://doi.org/10.1021/ja0105921.

(39)   García, Y. R.; Zelenka, J.; Pabon, Y. V.; Iyer, A.; Buděšínský, M.; Kraus, T.; Edvard Smith, C. I.; Madder, A. Cyclodextrin-Peptide Conjugates for Sequence Specific DNA Binding. *Org. Biomol. Chem.* **2015**, *13* (18), 5273–5278. https://doi.org/10.1039/c5ob00609k.

(40)   Castro, V.; Rodríguez, H.; Albericio, F. CuAAC: An Efficient Click Chemistry Reaction on Solid Phase. *ACS Comb. Sci.* **2016**, *18* (1), 1–14. https://doi.org/10.1021/acscombsci.5b00087.

(41)   Bush, C. A.; Sarkar, S. K.; Kopple, K. D. Circular Dichroism of (β Turns in Peptides

and Proteins. *Biochemistry* **1978**, *17* (23), 4951–4954. https://doi.org/10.1021/bi00616a015.

(42) Capito, R. M.; Azevedo, H. S.; Velichko, Y. S.; Mata, A.; Stupp, S. I. Self-Assembly of Large and Small Molecules into Hierarchically Ordered Sacs and Membranes. *Science (80-.).* **2008**, *319* (5871), 1812–1816. https://doi.org/10.1126/science.1154586.

(43) Aluri, S.; Pastuszka, M. K.; Moses, A. S.; MacKay, J. A. Elastin-like Peptide Amphiphiles Form Nanofibers with Tunable Length. *Biomacromolecules* **2012**, *13* (9), 2645–2654. https://doi.org/10.1021/bm300472y.

(44) Chen, R.; Shelby, S. A.; Zuckermann, R. N.; Mesch, R. A.; Kisielowski, C.; Nam, K. T.; Chu, T. K.; Tan, L.; Choi, P. H.; Connolly, M. D.; Marciel, A. B.; Lee, B.-C. Free-Floating Ultrathin Two-Dimensional Crystals from Sequence-Specific Peptoid Polymers. *Nat. Mater.* **2010**, *9* (5), 454–460. https://doi.org/10.1038/nmat2742.

(45) Ozkan, A. D.; Tekinay, A. B.; Guler, M. O.; Tekin, E. D. Effects of Temperature, PH and Counterions on the Stability of Peptide Amphiphile Nanofiber Structures. *RSC Adv.* **2016**, *6* (106), 104201–104214. https://doi.org/10.1039/c6ra21261a.

(46) Lange, S. C.; Unsleber, J.; Drücker, P.; Galla, H. J.; Waller, M. P.; Ravoo, B. J. PH Response and Molecular Recognition in a Low Molecular Weight Peptide Hydrogel. *Org. Biomol. Chem.* **2015**, *13* (2), 561–569. https://doi.org/10.1039/c4ob02069c.

(47) Yang, C.; Li, D.; Liu, Z.; Hong, G.; Zhang, J.; Kong, D.; Yang, Z. Responsive Small Molecular Hydrogels Based on Adamantane-Peptides for Cell Culture. *J. Phys. Chem. B* **2012**, *116* (1), 633–638. https://doi.org/10.1021/jp209441r.

(48) Carrazana, J.; Jover, A.; Meijide, F.; Soto, V. H.; Tato, J. V. Complexation of Adamantyl Compounds by β-Cyclodextrin and Monoaminoderivatives. *J. Phys. Chem. B* **2005**, *109* (19), 9719–9726. https://doi.org/10.1021/jp0505781.

(49) Kazantsev, R. V.; Tantakitti, F.; Zandi, R.; Yu, T.; Boekhoven, J.; Stupp, S. I.; Ortony, J. H.; Schatz, G. C.; Li, J.; de la Cruz, M. O.; Newcomb, C. J.; Shekhawat, G. S.; Wang, X.; Zhuang, E.; Palmer, L. C. Energy Landscapes and Functions of Supramolecular Systems. *Nat. Mater.* **2016**, *15* (4), 469–476. https://doi.org/10.1038/nmat4538.

(50) Sato, K.; Ji, W.; Palmer, L. C.; Weber, B.; Barz, M.; Stupp, S. I. Programmable Assembly of Peptide Amphiphile via Noncovalent-to-Covalent Bond Conversion. *J. Am. Chem. Soc.* **2017**, *139* (26), 8995–9000. https://doi.org/10.1021/jacs.7b03878.

(51) Pashuck, E. T.; Cui, H.; Stupp, S. I. Tuning Supramolecular Rigidity of Peptide Fibers through Molecular Structure. *J. Am. Chem. Soc.* **2010**, *132* (17), 6041–6046. https://doi.org/10.1021/ja908560n.

(52) Greenfield, M. A.; Hoffman, J. R.; De La Cruz, M. O.; Stupp, S. I. Tunable Mechanics of Peptide Nanofiber Gels. *Langmuir* **2010**, *26* (5), 3641–3647. https://doi.org/10.1021/la9030969.

(53) Khalily, M. A.; Goktas, M.; Guler, M. O. Tuning Viscoelastic Properties of Supramolecular Peptide Gels via Dynamic Covalent Crosslinking. *Org. Biomol. Chem.* **2015**, *13* (7), 1983–1987. https://doi.org/10.1039/c4ob02217c.

(54) Anderson, J. M.; Andukuri, A.; Lim, D. J.; Jun, H. W. Modulating the Gelation Properties of Self-Assembling Peptide Amphiphiles. *ACS Nano* **2009**, *3* (11), 3447–3454. https://doi.org/10.1021/nn900884n.

(55) Inostroza-Brito, K. E.; Collin, E.; Siton-Mendelson, O.; Smith, K. H.; Monge-Marcet, A.; Ferreira, D. S.; Rodríguez, R. P.; Alonso, M.; Rodríguez-Cabello, J. C.; Reis, R. L.; Sagués, F.; Botto, L.; Bitton, R.; Azevedo, H. S.; Mata, A. Co-Assembly, Spatiotemporal Control and Morphogenesis of a Hybrid Protein-Peptide System. *Nat. Chem.* **2015**, *7* (11), 897–904. https://doi.org/10.1038/nchem.2349.

(56)   Hedegaard, C. L.; Collin, E. C.; Redondo-Gómez, C.; Nguyen, L. T. H.; Ng, K. W.; Castrejón-Pita, A. A.; Castrejón-Pita, J. R.; Mata, A. Hydrodynamically Guided Hierarchical Self-Assembly of Peptide–Protein Bioinks. *Adv. Funct. Mater.* **2018**, *28* (16), 1–13. https://doi.org/10.1002/adfm.201703716.

(57)   Paramonov, S. E.; Jun, H. W.; Hartgerink, J. D. Modulation of Peptide-Amphiphile Nanofibers via Phospholipid Inclusions. *Biomacromolecules* **2006**, *7* (1), 24–26. https://doi.org/10.1021/bm050798k.

(58)   Stendahl, J. C.; Rao, M. S.; Guler, M. O.; Stupp, S. I. Intermolecular Forces in the Self-Assembly of Peptide Amphiphile Nanofibers. *Adv. Funct. Mater.* **2006**, *16* (4), 499–508. https://doi.org/10.1002/adfm.200500161.

(59)   Li, G.; Wu, J.; Wang, B.; Yan, S.; Zhang, K.; Ding, J.; Yin, J. Self-Healing Supramolecular Self-Assembled Hydrogels Based on Poly(l -Glutamic Acid). *Biomacromolecules* **2015**, *16* (11), 3508–3518. https://doi.org/10.1021/acs.biomac.5b01287.

(60)   Appel, E. A.; Forster, R. A.; Rowland, M. J.; Scherman, O. A. The Control of Cargo Release from Physically Crosslinked Hydrogels by Crosslink Dynamics. *Biomaterials* **2014**, *35* (37), 9897–9903. https://doi.org/10.1016/j.biomaterials.2014.08.001.

(61)   Shin, J.-W.; Mooney, D. J. Extracellular Matrix Stiffness Causes Systematic Variations in Proliferation and Chemosensitivity in Myeloid Leukemias. *Proc. Natl. Acad. Sci.* **2016**, *113* (43), 12126–12131. https://doi.org/10.1073/pnas.1611338113.

(62)   Engler, A. J.; Sen, S.; Sweeney, H. L.; Discher, D. E. Matrix Elasticity Directs Stem Cell Lineage Specification. *Cell* **2006**, *126* (4), 677–689. https://doi.org/10.1016/j.cell.2006.06.044.

(63)   Palmer, L. C.; Weber, B.; Ji, W.; Barz, M.; Sato, K.; Stupp, S. I. Programmable Assembly of Peptide Amphiphile via Noncovalent-to-Covalent Bond Conversion. *J.*

Am. Chem. Soc. **2017**, *139* (26), 8995–9000. https://doi.org/10.1021/jacs.7b03878.

(64) Lee, O.-S.; Stupp, S. I.; Schatz, G. C.; Matson, J. B.; Boekhoven, J.; Newcomb, C. J.; Sur, S.; Yu, J. M.; Ortony, J. H. Cell Death versus Cell Survival Instructed by Supramolecular Cohesion of Nanostructures. *Nat. Commun.* **2014**, *5* (1), 1–10. https://doi.org/10.1038/ncomms4321.

For Table of Contents Only